PHYSICAL REVIEW B VOLUME 19, NUMBER 4 15 FEBRUARY 1979

Multiple-scattering theory of intensities in inelastic-electron-tunneling spectroscopy

John Kirtley
IBM Thomas J. Watson Research Center, P.O. Box 218, Yorktown Heights, New York 10598

Paul Soven
Department of Physics, University of Pennsylvania, Philadelphia, Pennsylvania 19174

(Received 16 June 1978)

A short-range multiple-scattering theory of the observed intensities in inelastic-electron-tunneling spectroscopy (IETS) is developed and compared with previous long-range theories. The scattering molecular potential is calculated using the $X\alpha$ approximation to the exchange-correlation potential and the Bardeen transfer-Hamiltonian approach is taken to calculate inelastic-tunneling cross sections. Predicted short-range cross sections are strongly energy dependent and could be quite large for tunneling electrons at a molecular bound-state energy. However, comparison of the predictions of the two theories for higher-harmonic amplitudes and opposite-bias-voltage asymmetries indicates that the long-range interactions dominate in IETS.

Inelastic-electron-tunneling spectroscopy (IETS)[1-3] is a sensitive technique for measuring the vibrational spectra of molecules adsorbed on the oxide surface of metal-oxide-metal tunneling junctions. In this technique, peaks in the second derivative of the current-voltage characteristics (d^2I/dV^2 vs V) of these junctions appear at voltages V_i given by the quantum relation $eV_i = \hbar\omega_i$, where ω_i are the vibrational frequencies of the absorbed molecules. These peaks occur because of small increases in the conductance of the junction due to the presence of additional tunneling channels when the bias voltage exceeds the inelastic threshold. When $eV > eV_i = \hbar\omega_i$, electrons can tunnel inelastically, losing energy to a vibrational excitation of the molecule, and still find empty final states in the second electrode. The positions (in energy) of the peaks give information about the structure and bonding of the molecules on the oxide surface. Recently, there has been a great deal of interest in the amplitudes of the peaks, which may, for example, give information about the orientation of the molecules on the surface.

Previous treatments of intensities in IETS[4,5] have used simple model potentials that have been essentially long range in nature. These treatments assumed that the primary interaction of the tunneling electron is with the intrinsic or induced dipole moments of the vibrating molecule. One major objection to these treatments is that they ignore the contribution of the short-range part of the molecular potential to the inelastic-tunneling process. We present here for the first time calculations of the short-range contributions to IETS intensities. Comparisons of the predictions of our short-range model and previous long-range models with experimental measurements of (a) relative intensities for opposite-bias polarities and (b) higher harmonic intensities indicate that the long-range interactions dominate in inelastic electron tunneling. This conclusion clears the way for a more confident detailed comparison of the long-range theory with experiment.

The calculations to be described in this paper employed the multiple-scattering $X\alpha$ approach,[6,7] which has enjoyed some success in applications in the area of surface spectroscopies.[8] In this formulation, the molecular potential for fixed nuclear positions $\vec{R}_N$ is given by

$$V_{x\alpha}(\vec{r}, \vec{R}_N) = V_H(\vec{r}) + V_N(\vec{r}, \vec{R}_N) + V_{xc}(\vec{r}) . \qquad (1)$$

The static electron-electron interaction or Hartree term is given by

$$V_H(\vec{r}) = \int \frac{d^3r' e^2 n(\vec{r}\,')}{|\vec{r} - \vec{r}\,'|} , \qquad (2)$$

where $n(\vec{r}\,')$ is the electron density at position $\vec{r}\,'$. The nuclear-attraction term is given by

$$V_N(\vec{r}, \vec{R}_N) = \sum_N \frac{-Z_N e^2}{|\vec{R}_N - \vec{r}|} , \qquad (3)$$

where Z_N is the screened nuclear charge. The exchange-correlation term is approximated by

$$V_{xc}(\vec{r}) = -3\alpha e^2[3n(\vec{r})/8\pi]^{1/3} , \qquad (4)$$

where α is a parameter of order 0.7. In the muffin-tin approximation the molecular potential is spherically averaged within spheres centered on the individual atoms in the molecule, and outside an outer sphere surrounding the molecule. The intersphere region is volume averaged. An initial guess is made for the molecular potential, the wave functions are found by numerical integration and matching wave functions at the muffin-tin boundaries, and the potential is recalculated, iterating to convergence. Finally, the molecular potential found using this procedure is exponentially attentuated at large distances and replaced with a polarizability potential (as discussed in Davenport, Ho, and Schrieffer[9]) to fit gas-phase inelastic-electron-scattering data better.

The molecular potential found in this way was placed a distance a from one metal electrode in a metal-insulator-metal sandwich geometry with insulator thickness l [Fig. 1(a)]. Since the $X\alpha$ potential falls off rapidly with distance, we placed a sphere of radius R on the molecule, within which the potential was made up of both the barrier oxide potential and the $X\alpha$ molecular potential. Outside the sphere the total potential was given by the oxide potential. The actual value of R drops out of the calculations, so one need only assume that there is some R for which the oxide potential dominates (for CO, $V_{x\alpha} = -0.064$ eV at $R = 2$ Å, much smaller than the oxide potential of ~2 eV). It seems reasonable to assume that the one electron potential in the vicinity of the molecule is simply the sum of the gas-phase molecular potential and the barrier potential. In the language of the muffin-tin approximation this means that the position of the muffin-tin constant with respect to the top of the barrier for the oxide-embedded molecule is equal to its position with respect to the vacuum level for the gas-phase molecule. Once the barrier height is chosen, this assumption determines the energy of the tunneling electron with respect to the mean molecular potential. Rather than be constrained by this assumption we have chosen to calculate the inelastic current for a range of possible tunneling energies measured with respect to the mean molecular potential. In this way we are able to discuss both resonant and nonresonant tunneling; we find, as discussed below, that the character of the inelastic-tunneling current depends critically upon the value of this energy.

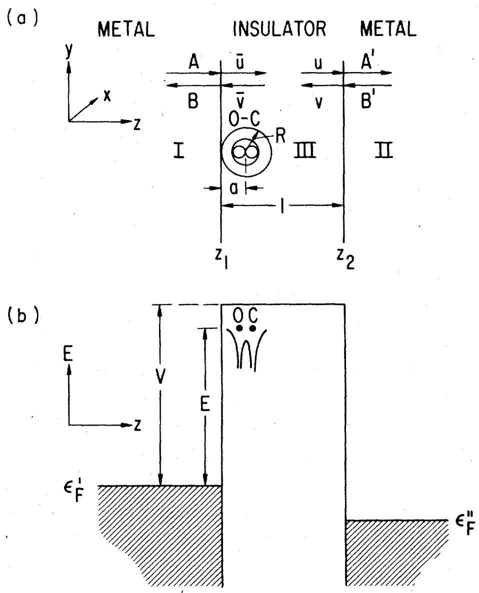

FIG. 1. Assumed tunneling junction geometry (a) in cross section and (b) in energy as a function of z.

The inelastic-tunneling matrix element is calculated by combining the Born-Oppenheimer principle with standard multiple scattering and transfer Hamiltonian techniques. Much of the formalism is similar to that employed by Pendry[10] in his layer KKR techniques and by Davenport, Ho, and Schrieffer[9] in their study of gas-phase inelastic scattering. It is easily shown that, in the Born-Oppenheimer approximation, the amplitude for inelastic tunneling is proportional to the matrix element of the elastic scattering amplitude (as a function of the molecular geometry) between the appropriate vibrational wave functions.

The tunneling matrix element is calculated for a given internuclear spacing by matching wave functions across all boundaries. The wave functions in region I (see Fig. 1) can be expanded in plane-wave states as

$$\psi_1 = \int d^2k_\parallel [A(k_\parallel)\exp(i\vec{k}_\parallel \cdot \vec{r}_\parallel)\exp ik_z z + B(k_\parallel)\exp(i\vec{k}_\parallel \cdot \vec{r}_\parallel)\exp(-ik_z z)], \qquad (5)$$

with a similar expression for region II. The wave function just inside the oxide region (but outside the molecular sphere) at $z = z_1$ is expanded in decaying plane waves:

$$\Psi_{\mathrm{III}}(\vec{r}, z = z_1) = \int d^2k_\parallel [\bar{u}(k_\parallel)e^{i\vec{K}^+ \cdot \vec{r}} + \bar{v}(k_\parallel)e^{i\vec{K}^- \cdot \vec{r}}], \qquad (6)$$

where

$$\vec{K}^\pm = k_x\hat{x} + k_y\hat{y} \pm iQ\hat{z}, \quad Q = [(2m/\hbar^2)(U - \epsilon - k_\parallel^2)]^{1/2}, \qquad (7)$$

with a similar expression at $z = z_2$. The wave function on the sphere boundary (at $r = R$) can be expanded in spherical harmonics:

$$\Psi_{\mathrm{sp}}(|\vec{r}| = R) = \sum_\lambda A_\lambda \left(k_\lambda^{(1)}(kR)Y_\lambda(\hat{r}) + \sum_L S_{\lambda L} k_L^{(2)}(kR) Y_L(\hat{r}) \right), \qquad (8)$$

where (using Johnson's[7] notation)

$$k=\left[(2m/\hbar^2)(U-\epsilon)\right]^{1/2},\quad k_\lambda^{1,2}(kR)=-i^{-\lambda}h_\lambda^{1,2}(kR), \tag{9}$$

$h_\lambda^{1,2}(kR)$ are spherical hankel functions, $Y_L(\hat{r})=Y_{l,m}(\hat{r})$ are spherical harmonics, and the sums λ and L are taken over all l and m indices.

Matching boundary conditions at $|\vec{r}|=R$, $z=z_1$, and $z=z_2$ are most easily accomplished by finding the general expression for the wave function in region III using Green's theorem:

$$\Psi(\vec{r})=\oint ds'\left(\Psi(\vec{r}')\frac{\partial G(\vec{r},\vec{r}')}{\partial n'}-G(\vec{r},\vec{r}')\frac{\partial\Psi(\vec{r}')}{\partial n'}\right). \tag{10}$$

The Green's-function expansion in spherical harmonics is

$$G(\vec{r},\vec{r}')=-ik\sum_L Y_L(\hat{r})Y_L(\hat{r}')j_l(kr_<)h_l^{(1)}(kr_>), \tag{11}$$

while in plane-wave expansion one obtains

$$G(\vec{r},\vec{r}')=-\frac{1}{(2\pi)^3}\int d^3q\,\frac{e^{i\vec{q}\cdot(\vec{r}-\vec{r}')}}{k^2+q^2-i\delta}. \tag{12}$$

Summing the contributions to the surface integral in Eq. 10 from $z=z_1$, $z=z_2$, and $r=R$, we find that

$$\Psi_{\text{III}}(\vec{r})=\sum_{\lambda,L}A_\lambda(i^{-\lambda}\delta_{\lambda L}-i^{-1}S_{\lambda L})h_l^{(1)}(kr)Y_L(\hat{r})+\int d^2k_\parallel[\bar{u}(k_\parallel)e^{i\vec{K}^+\cdot\vec{r}}+v(k_\parallel)e^{i\vec{K}^-\cdot\vec{r}}]. \tag{13}$$

By comparing this expression with the expression for Ψ_{III} at $|\vec{r}|=R$ [Eq. (8)], and using the expansion

$$e^{i\vec{K}^\pm\cdot\vec{r}}=4\pi\sum_L i^l Y_L(\hat{r})Y_L(\hat{K}^\pm)j_l(kr), \tag{14}$$

we find that

$$A_\lambda=-2\pi\sum_{\lambda'}(-1)^{\lambda'}S^{-1}_{\lambda\lambda'}\int d^2k_\parallel[Y_{\lambda'}(K^+)\bar{u}(k_\parallel)+Y_{\lambda'}(K^-)v(k_\parallel)]. \tag{15}$$

Similarly, by comparing Eq. (13) with the expressions for Ψ_{III} at $z=z_1$, and $z=z_2$ and using the expansion

$$-iY_L(\hat{r})h_l^{(1)}(kr)=\frac{1}{(2\pi)^2}\int d^2k_\parallel\frac{e^{i\vec{k}_\parallel\cdot\vec{r}_\parallel}(-2\pi i)i^{-l}}{kQ}\times\begin{cases}Y_L(\vec{K}^+)e^{iQZ}, & z>0\\ Y_L(\vec{K}^-)e^{-iQZ}, & z<0\end{cases} \tag{16}$$

we find that

$$u(k_\parallel)=\bar{u}(k_\parallel)+\frac{1}{2\pi kQ}\sum_{\lambda L}A_\lambda(S_{\lambda L}-\delta_{\lambda L})(-1)^l Y_L(\vec{K}^+),$$

$$\bar{v}(k_\parallel)=v(k_\parallel)+\frac{1}{2\pi kQ}\sum_{\lambda L}A_\lambda(S_{\lambda L}-\delta_{\lambda L})(-1)^l Y_L(\vec{K}^-). \tag{17}$$

In Eqs. (14)–(17) the functions $Y_L(\vec{K}^\pm)$ of complex arguments are unambiguously defined by expressing the spherical harmonics in terms of the Cartesian coordinates k_x/k, k_y/k, and iQ/k and substituting in the corresponding complex values. One can see from the form of Eqs. (15)–(17) that the scattering is defined for a given junction geometry by the scattering matrices $S_{\lambda L}$, which are functions of internuclear spacing and incident electronic energy. The S matrices were found by solving the Schrödinger equation for a scattering state of negative energy $-E$ in the presence of the $X\alpha$ potential, using the procedure followed for finding molecular wave function.

The system of equations (15) and (17) represent a complete solution of the tunneling wave function inside the oxide barrier. Matching boundary conditions to incoming and outgoing plane waves of the form of Eq. (5) would in principle give an exact expression for the tunneling matrix element. However, this approach would be quite complex and time consuming. A substantial simplification of the problem can be made by using the Bardeen tunneling formalism. Consider left to right tunneling. In the Bardeen picture the initial wave function is calculated by extending the right-hand side of the oxide barrier to $+\infty$. This is equivalent to setting $v(k_\parallel)=0$. The final wave function is similarly calculated by setting $\bar{u}(k_\parallel)=0$. The correctly normalized coefficients of an initial plane-wave state with wave vector $k'_\parallel$ and a final plane-wave state with wave vector $k''_\parallel$ parallel to the interface are

$$\bar{u}_0(k_\parallel)=\gamma_Z e^{i(k_z-Q)z_1}\delta(k_\parallel-k'_\parallel),$$

$$v_0(k_\parallel)=\gamma_Z e^{i(k_z+Q)z_2}\delta(k_\parallel-k''_\parallel),$$

$$\gamma_Z=\frac{(1/\sqrt{2}L^{3/2})k_z}{k_z+Q}, \tag{18}$$

where the normalization is done in a cube of side L. Substituting these expressions into Eqs. (13), (15), and (17) and using the Bardeen expression for the tunneling matrix element,

$$M_{k'k''}=\frac{-\hbar^2}{2m}\int dxdy(\Psi^L_{k'}\partial\Psi^{R*}_{k''}/\partial z-\Psi^{R*}_{k''}\partial\Psi^L_{k'}/\partial z)_{z=z_2}, \tag{19}$$

we find the following expression for the total matrix element:

$$M_{k'k''} = (4\pi^2\hbar^2 i/m)\gamma_Z'\gamma_Z''^{*}Q'' \times\{(-1)^{\lambda'-l}Y_{\lambda'}(\vec{K}^{+\prime})S^{-1}_{\lambda'\lambda}(S_{\lambda L}-\delta_{\lambda L}) \times Y_L(\vec{K}^{+\prime\prime})e^{i(k_Z'-Q')z_1}e^{-i(k_Z''-Q'')z_2}/k''Q''\} \tag{20}$$

(we follow the convention that repeated indices are summed over). The inelastic matrix element is approximately given by

$$M^i_{k'k''} = \langle \nu | M_{k'k''} | 0\rangle , \tag{21}$$

where $|0\rangle$ and $|\nu\rangle$ are, respectively, the ground and relevant excited vibrational wave functions of the molecule and $M_{kk'}$ is a function of the molecular coordinates.

If we define the inelastic T matrix element as

$$T^i_{\lambda L} = (-1)^{\lambda-l}\langle \nu | S^{-1}_{\lambda\lambda'}(\delta_{\lambda' L}S_{\lambda' L})|0\rangle , \tag{22}$$

we obtain for the inelastic matrix element squared

$$|M^i_{k'k''}|^2 = \frac{16\pi^4\hbar^4}{m^2}\,\frac{|\gamma'_Z|^2|\gamma''_Z|^2}{k''^2} \times [Y_{\lambda'}(\vec{K}^{+\prime})Y^*_{\lambda}(\vec{K}^{+\prime})T^i_{\lambda' L}T^i_{\lambda L'}Y_L(\vec{K}^{+\prime\prime}) \times Y^*_{L'}(\vec{K}^{+\prime\prime})e^{-2iQ'z_1}e^{2iQ''z_2}] . \tag{23}$$

The total inelastic current through the junction is found by summing over all initial and final states using Fermi's golden rule:

$$j_i = \frac{4\pi e}{\hbar}\sum_{k'}\sum_{k''} |M^i_{k'k''}|^2 f(\epsilon_{k'})[1-f(\epsilon_{k''}+eV)] \times N_1(\epsilon_{k'})N_2(\epsilon_{k''}+eV)\delta(\epsilon_{k'}-\epsilon_{k''}+\hbar\omega) \tag{24}$$

We assume for simplicity a δ-function spectral weight function for the vibrational frequencies, since we are interested in the integrated intensity rather than the specific line shape. Similarly we assume that the metal electrodes are normal so that the tunneling density of states functions N_1 and N_2 can be taken to be constants. Superconducting electrodes affect the observed line shapes, but not the integrated intensities. The Fermi functions take the form shown because at low temperatures the molecules are in their vibrational ground state and only inelastic tunneling with electrons losing energy is allowed. Taking the low-temperature form for the Fermi functions

$$f(\epsilon) \xrightarrow[T\to 0]{} 1-\Theta(\epsilon)$$

and taking two derivatives of (24), we find

$$\frac{d^2 j_i}{d(eV)^2} = \frac{8\pi e}{\hbar}\left(\frac{L}{\pi}\right)^6\left(\frac{m}{\hbar^2}\right)^3(\epsilon'_F)^{1/2}(\epsilon''_F+eV)^{1/2}\int_0^{2\pi}d\phi'\int_0^{2\pi}d\phi''\int_0^1 d(\cos\theta')\int_0^1 d(\cos\theta'')\,|M^i_{k'k''}|^2\delta(\hbar\omega-eV) , \tag{25}$$

where the matrix element is evaluated with initial and final electron energies on the Fermi surface (which is assumed spherical).

The integrations over solid angle can be conveniently separated by writing

$$\int d\Omega'\int d\Omega''|M^i_{k'k''}|^2 = \frac{16\pi^2\hbar^4}{m^2k^2}\alpha_{\lambda'\lambda}\beta_{LL'}T^i_{\lambda' L}T^i_{\lambda L'} , \tag{26}$$

with

$$\alpha_{\lambda'\lambda} = \int d\Omega'\,|\gamma'_Z|^2 Y_{\lambda'}(\vec{K}^{+\prime})Y^*_{\lambda}(\vec{K}^{+\prime})e^{-2iQ'z_1},$$

$$\beta_{LL'} = \int d\Omega''\,|\gamma''_Z|^2 Y_L(\vec{K}^{+\prime\prime})Y^*_{L'}(\vec{K}^{+\prime\prime})e^{2iQ''z_2} . \tag{27}$$

The change in total conductance due to the excitation of a given vibrational mode per molecule/(unit area) is given by

$$\frac{\Delta\sigma}{n} = \int d(eV)\frac{d^2 j_i}{d(eV)^2} , \tag{28}$$

where n is the surface density of molecular scatterers. A convenient expression to compare with experiment is obtained by dividing (28) by the total conductance of the junction predicted using the same square barrier as above:

$$\sigma = \frac{e}{(2\pi)^2\hbar l^2}\left(\frac{2m(U-\epsilon_F)}{\hbar^2}\right)^{1/2}e^{-2l}\left(\frac{2m}{\hbar^2}(U-\epsilon_F)\right)^{1/2} . \tag{29}$$

The inelastic cross section is then $\Delta\sigma/n\sigma$, and the ratio of the change in conductance divided by the total conductance is obtained by multiplying by n. The angular integrations in (27), the evaluations of the spherical harmonics of imaginary arguments, the evaluation of the S matrices, and the summation of (26) were all done numerically. In all cases we assumed $V=2$ eV and $l=20$ Å. The ratio of inelastic to elastic conductances does not depend strongly on these parameters.

We have employed this formalism to study the inelastic tunneling current when CO is imbedded in the oxide layer. The potential describing the molecule was the one used by Davenport *et al.*[9] in their study of gas-phase scattering. There is no reason why exactly the same molecular potential is appropriate to these two very different situations; fortunately, the nature of the conclusions we draw is independent of the details of the potential. For completeness we mention that the potential is that of a CO molecule with one-half additional electron. This generalization[9] of the transition-state method was meant to simulate the short-range polarization processes that presumably occur during the scattering process. The potential smoothly approaches the standard polarization form $1/r^4$ in the outer regions of the molecule; again the details do not effect our conclusions. The angular-momentum expansions were truncated at $l=2$ for the atomic spheres and at $l=3$ for the outer sphere.

Figure 2 shows the predicted inelastic cross sections for the $\nu=0$ to $\nu=1$ transition for CO as a function of the assumed orientation of the molecules on the surface, for three different tunneling energies. In these polar plots the point at 0° (vertically upward) corresponds to CO oriented normal to the oxide surface with the carbon atom down. The orientation dependence of the cross section does not depend strongly on tunneling electron energy. However, the dependence of the amplitude of the cross section on tunneling energy is quite strong, peaking at $E=-1.8$ eV.

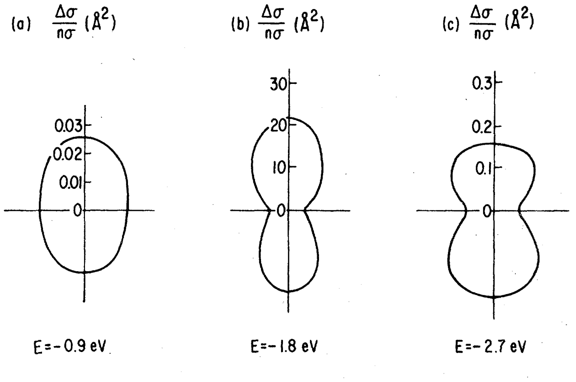

FIG. 2. Predicted $X\alpha$ first-harmonic cross section for CO as a function of assumed orientation on the surface, for three different tunneling energies. Vertically upward (0°) corresponds to CO oriented normal to the oxide surface with the carbon atom down. The cross sections are strongly dependent on tunneling energy, reaching a resonance of $E=-1.8$ eV.

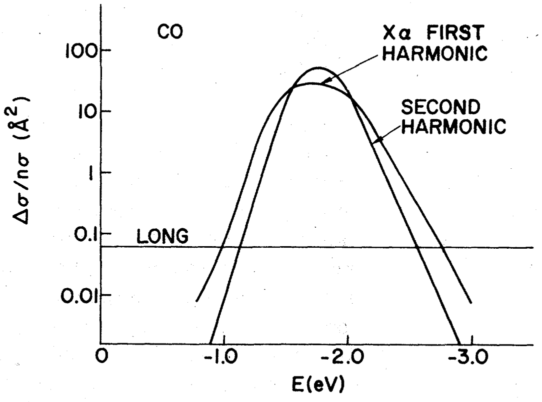

FIG. 3. Predicted $X\alpha$ inelastic first-and second-harmonic cross sections for CO as a function of energy, compared with long-range (KSH) theory. The predicted $X\alpha$ cross sections become large near a bound-state energy, but the ratio of second- to first-harmonic intensities becomes much larger than when observed experimentally.

Figure 3 shows the predicted inelastic cross sections for both first- and second-harmonic transitions as a function of the energy of the tunneling electron with respect to the vacuum level of the molecule, assuming CO orientation normal to the interface with the carbon atom down. There is a bound-state energy level 1.8 eV below the vacuum for the $X\alpha$ potential used. When the tunneling electron matches the bound-state energy, the predicted first-harmonic intensity is greatly enhanced. The crucial point, however, is that the second-harmonic cross section increases also, so that at resonance the second-harmonic term is as large as the first-harmonic term. Included for comparison is the predicted cross section for the long-range theory of Kirtley, Scalapino, and Hansma[5] (KSH) (which is independent of energy, assuming CO orientation normal to the interface, an oxide dielectric constant of 3, an rms displacement of 0.034 Å, and a dipole derivative of $1.32e$. Direct comparison of these cross sections with experiment is difficult, since the absolute surface densities are not yet known. (The experiments of Hansma, Kaska, and Laine for CO on Rh-doped alumina give values for $\Delta\sigma/\sigma$ of 0.1%, which would indicate a surface density of 0.016 $l/\text{Å}^2$ if the long-range cross section dominated. This is a factor of ~3 smaller than one might expect from a close-packed square array of hard spheres.) However, comparison of the long-range with the short-range cross sections shows that the long range dominates off resonance, and that on resonance higher harmonic excitations should be seen. Experimentally, the second-harmonic intensities are very small[11] (~200 times smaller than the first-harmonic intensities for benzoic acid on alumina), much smaller than would be expected if resonant scattering played an important role in IETS. Note that these conclusions are not dependent on the assumed orientation of the CO molecules on the surface: for example, for CO oriented parallel to the surface the KSH cross section is reduced by a factor of 10; off resonance the short-range cross section is reduced by a factor of ~2; and the long-range cross section still dominates except near resonance, where higher harmonic components would be expected.

A second clue to the relative contributions of the long- and short-range interactions in IETS comes from measurements of the ratio of intensities for opposite-bias voltages. For Al-AlO$_x$-Rh-Co-Pb tunneling junctions the intensity of the CO stretch mode is smaller for Al biased positive then for Al biased negative: the ratio $(\Delta\sigma/\sigma^+)/(\Delta\sigma/\sigma^-)$ is ~0.68. The reason for this asymmetry is clear: for Al negative the electron tunnels through the oxide before interacting with the CO on the surface and losing energy, but for Al positive the electron must tunnel after losing energy. The asymmetry results since less energetic electrons are less likely to penetrate the barrier. A short-range interaction could be expected to predict a large asymmetry, since the interaction is localized close to one electrode, but a long-range interaction would give less asymmetry. This is indeed the case: the calculation described here predicts an asymmetry ratio of 0.23, while the long-range (KHS) theory gives 0.59, in better agreement with the experimental value of 0.68.

In conclusion, we have calculated for the first time the contributions of the short-range interactions to intensities in IETS. Experimental observations of very small second-harmonic intensities, and relatively small opposite-bias-voltage asymmetries in intensities, indicate that the long-range interactions dominate in IETS.

We would like to thank J. W. Davenport for the loan of his computer programs and a great deal of advice and assistance, and J. R. Schrieffer and W. Ho for useful conversations. This research was partially supported by the National Science Foundation under Grants No. DMR 73-024S4A01 and No. DMR-77-23420 and by Materials Research Laboratories Program Grant No. DMR 76-00678.

---

[1] R. C. Jaklevic and J. Lambe, Phys. Rev. Lett. 17, 1139 (1966); J. Lambe and R. C. Jaklevic, Phys. Rev. 165, 821 (1968).

[2] P. K. Hansma, Phys. Rep. 30C, 145 (1977).

[3] P. K. Hansma and John Kirtley, Acc. Chem. Res. (to be published).

[4] D. J. Scalapino and S. M. Marcus, Phys. Rev. Lett. 18, 459 (1967).

[5] J. Kirtley, D. J. Scalapino, and P. K. Hansma, Phys. Rev. B 14, 3177 (1976).

[6] J. C. Slater, Adv. Quantum Chem. 6, 1 (1972).

[7] K. H. Johnson, Adv. Quantum Chem. 7, 143 (1973).

[8] J. W. Davenport, Phys. Rev. Lett. 36, 945 (1976).

[9] J. W. Davenport, W. Ho, and J. R. Schrieffer, Phys. Rev. B 17, 3115 (1978).

[10] J. B. Pendry, Surf. Sci. 57, 679 (1976).

[11] Richard Kroeker (private communication).